AJNR

Chiari II Malformation: MR Imaging Evaluation

Samuel M. Wolpert, Mary Anderson, R. Michael Scott, Eddie S. K. Kwan and Val M. Runge

AJNR Am J Neuroradiol 1987, 8 (5) 783-792
http://www.ajnr.org/content/8/5/783

Chiari II Malformation: MR Imaging Evaluation

Samuel M. Wolpert[1]
Mary Anderson[1]
R. Michael Scott[2]
Eddie S. K. Kwan[1]
Val M. Runge[3]

The purpose of this study was to explore the value of high-detail MR imaging in the diagnosis of the Chiari II malformation. Twenty-four patients with known Chiari II malformation as diagnosed by CT scanning were evaluated with cranial MR scans. Two patients also had spine scans. The sagittal-plane images were the most informative, and abnormalities of the telencephalon, diencephalon, mesencephalon, rhomboencephalon, upper spinal cord, and mesencephalon were shown extremely well.

We found MR to be an easy and accurate method for demonstrating the abnormalities of the Chiari II malformation, and it is our procedure of choice.

The Chiari II malformation is a complex developmental deformity characterized by an elongated small cerebellum and brainstem with caudal displacement of the medulla, parts of the cerebellum, and pons through an enlarged foramen magnum into the cervical spinal canal [1]. A meningomyelocele is a nearly constant accompanying feature, as is hydrocephalus. In addition, numerous other malformations of the neuraxis including polymicrogyria, subependymal heterotopias, beaked colicular plate, aqueduct stenosis, diastematomyelia, diplomyelia, hydromyelia, and syringomyelia have been reported [1].

We had the opportunity to evaluate 24 patients with Chiari II malformation with high-detail MR imaging. Most abnormalities previously described as seen by CT [2–5] were also seen by MR. In this article we review these abnormalities and report on other associated features of the Chiari malformation that either have a greater frequency than has previously been reported or that have not been described before.

Subjects and Methods

Twenty-four patients with meningomyeloceles and known Chiari II malformations as diagnosed by CT scanning were investigated with MR imaging. Three patients were less than 1 year old, five were 1–5 years old, five were 6–10 years old, and 11 were 10–20 years old. In 21 of the patients ventricular shunts had been inserted previously; in one patient a lumbar subarachnoid-peritoneal shunt had been placed. Sagittal and axial head images were obtained in all patients. The majority of the sagittal images (16) were 3 mm thick; the rest were either 4 or 5 mm thick. Eighteen patients had coronal scans (5–10 mm thick). Spin-echo techniques were used. Since the anatomy of the lesions was the prime consideration, mild T1-weighted images were obtained in all cases with a repetition time of 500, 600, or 800 msec and an echo time of 17 msec. T2-weighted images were not obtained routinely. In all patients, an attempt was made to include the upper cervical spine on the sagittal images. In addition, two patients had separate T1-weighted sagittal images of the spine, and one of the two had T2-weighted sequences as well.

Results

The results are categorized by the involvement of the different embryologic parts of the brain and are summarized in Table 1.

This article appears in the September/October 1987 issue of *AJNR* and the November 1987 issue of *AJR*.

Received December 16, 1986; accepted after revision March 13, 1987.

[1] Department of Radiology, Section of Neuroradiology, New England Medical Center Hospitals, 750 Washington St., Boston, MA 02111. Address reprint requests to S. M. Wolpert.

[2] Department of Neurosurgery, New England Medical Center Hospitals, Boston, MA 02111.

[3] Department of Radiology, Section of MR Imaging, New England Medical Center Hospitals, Boston, MA 02111.

***AJNR* 8:783–792, September/October 1987**
0195–6108/87/0805–0783

TABLE 1: MR Abnormalities in Chiari II Malformations

Location: Abnormality	No. of Patients (n = 24)
Telencephalon:	
Stenogyria	7
Frontal horn beaking[a]	11
Corpus callosum (partial agenesis)	8
Supracerebellar CSF-containing spaces	10
Third ventricle diverticulum	1
Diencephalon:	
Enlarged third ventricle	3
Large massa intermedia	16
Elevation of hypothalamus	2
Mesencephalon:	
Aqueduct not seen	17
Bulbous tectum	14
Beaked tectum	10
Rhomboencephalon	
Absent cerebellar folia	12
Superior vermis	9
Inferior vermis	10
Overlapping anterior cerebellar margins	18
Cerebellar vermial pegs	23
Cervicomedullary deformities[b]:	
Type 1	6
Type 2	7
Type 3a	8
Type 3b	3
Pyramidal hypogenesis	4
Spinal cord:	
Wide anterior space	9
Syrinx	3
Mesodermal:	
Clival scalloping	19
Gyral interdigitations (falx hypoplasia)	9
Wide incisura[c]	15
Gyral indentations (into skull)	8

[a] Twelve acceptable coronal scans of frontal horns.
[b] See text for elaboration.
[c] All 15 patients had overlapping anterior cerebellar margins.

Discussion

MR imaging is known to be superior to CT in demonstrating the craniovertebral junction, particularly the spinal cord, medulla, cerebellum, pons, and surrounding subarachnoid spaces, and MR is perhaps the best technique for demonstrating structural abnormalities of the Chiari II malformation. Although additional manifestations of the malformation such as aqueduct stenosis and massa intermedia enlargement are usually well defined by CT, MR demonstrates superior anatomic detail in these areas as well.

The MR images of our patients, in addition to duplicating previous CT findings, highlighted other components of the malformation that previously have not been emphasized or described in the radiologic or neuropathologic literature. Each of the areas is discussed separately.

Telencephalon

Stenogyria.—Small, closely spaced gyral folds were seen in seven patients, five of whom also had partial agenesis of the corpus callosum (Fig. 1). Although this finding is usually termed "polymicrogyria" and is described as occurring in about 50% of patients with the Chiari II malformation [6, 7], according to Muller [8] the cerebral cortex in patients with the Arnold-Chiari malformation is normal and should not be confused with true polymicrogyria, in which the cellular layers of the cortex are deficient. Muller used the term "stenogyria" to describe a histologically normal cortex thrown into innumerable small, closely spaced folds. Although we have no histologic verification of normal cortical architecture in our patients, this term appears to be more appropriate for the MR appearances of the cortical gyral pattern in these patients.

Anterior horns.—Anteroinferior pointing of the anterior horns was seen in 11 of the 12 patients in this series in whom coronal scans had been obtained through the frontal horns (Fig. 2). In one series these appearances were seen on ventriculograms in 32 of 62 patients with the Arnold-Chiari malformation [9]. The cause of the findings was thought to be either a medially directed force causing undue juxtaposition of the two cerebral hemispheres or marked inward bulging of the caudate nucleus [4, 9].

Corpus callosum.—Partial agenesis of the corpus callosum was seen in eight (33%) of the 24 patients (Figs. 1, 3, and 4). Six of these patients had medial radiating sulci on the inner surface of the adjacent parietal lobes. In another four patients marked thinning of the posterior portion of the body and the splenium of the corpus callosum was seen, possibly a result of previous severe hydrocephalus. Other associated features of agenesis of the corpus callosum, such as dysplasia or absence of the cingulate gyrus [10], were seen in six of the eight patients. Failure of the parietooccipital and calcarine fissures to converge was seen in six patients.

Agenesis of the corpus callosum in association with the Arnold-Chiari malformation has been described but not with this great a frequency. Gilbert et al. [11] described three cases of complete or nearly complete agenesis of the corpus callosum in a series of 25 autopsies of children with Arnold-Chiari malformations. Venes et al. [12] reported a case of partial agenesis of the corpus callosum demonstrated by MR, but the anomaly was not mentioned in the article. Two cases of the Chiari II malformation demonstrated by MR were found in a series of 11 patients with agenesis of the corpus callosum described by Atlas et al. [13]. The association between the two anomalies further emphasizes the fact that the Chiari II malformation involves not only the hindbrain but also other fiber tracts in the human brain.

The finding of a deformed corpus callosum on MR may be of some value in predicting intelligence in children with myelomeningoceles. Of the eight children with the anomaly, two are severely retarded and two require special schooling. One child appears to have a normal mental state, but is so disabled by extremity deficits and breathing difficulties that he cannot be tested easily. Only three appear to be developing normally with normal intelligence. The other 16 children without severe deformations of the corpus callosum all have normal or nearly normal intelligence.

Supracerebellar CSF-containing spaces (CCS).—Wide supracerebellar CCS involving to varying degrees the quadrigeminal plate cistern, the cistern velum interpositum, the interhemispheric fissure, and the ambient cistern were seen in 10 of the 24 patients (Figs. 3–5). In one other patient the

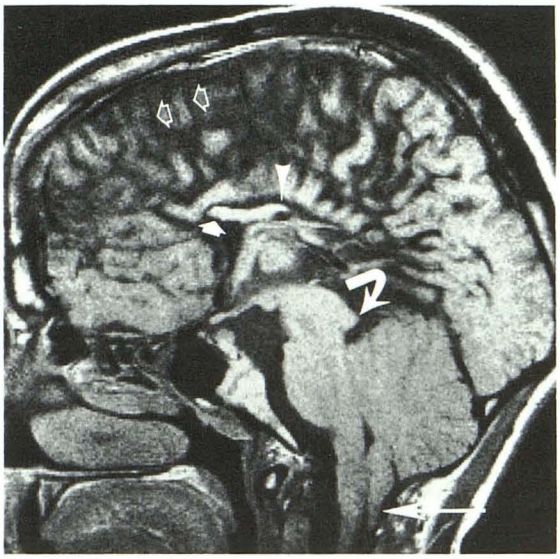

Fig. 1.—Multiple, closely spaced gyri (*open arrows*) are radially oriented. Posterior portion of body and splenium of corpus callosum are absent (*arrowhead*). Rostrum of corpus callosum is absent (*short solid arrow*). Aqueduct is not seen and inferior colliculus (*curved arrow*) has beaked appearance. Fourth ventricle is at level of foramen magnum and inferiorly is seen extending through foramen magnum anterior to inferior vermial peg (*long solid arrow*) (group 2a in text). Clivus is concave. An insufficient amount of upper cervical canal is included on scan to determine whether cervicomedullary kink is present also.

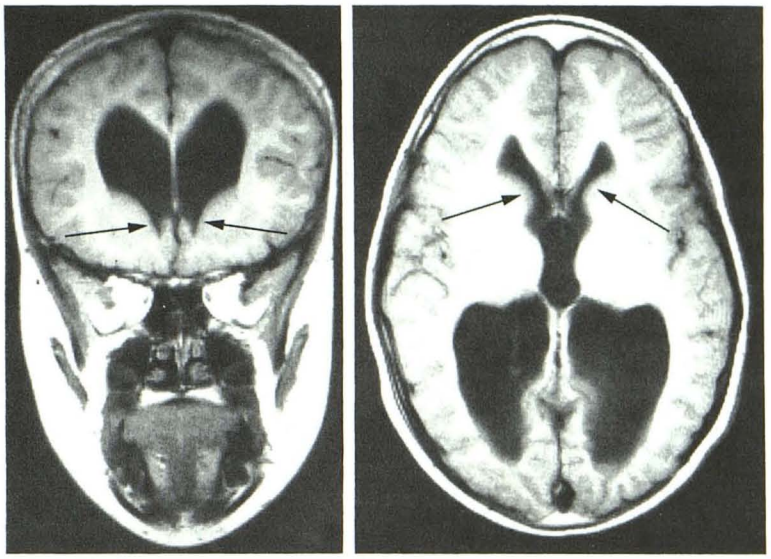

A B

Fig. 2.—*A*, Inferior pointing of lateral ventricular floor (*arrows*) is associated with enlarged anterior horns.

B, Heads of caudate nuclei (*arrows*) bulge medially into anterior horns. Note enlarged lateral ventricles and occipital horn. Third ventricle is unusually large.

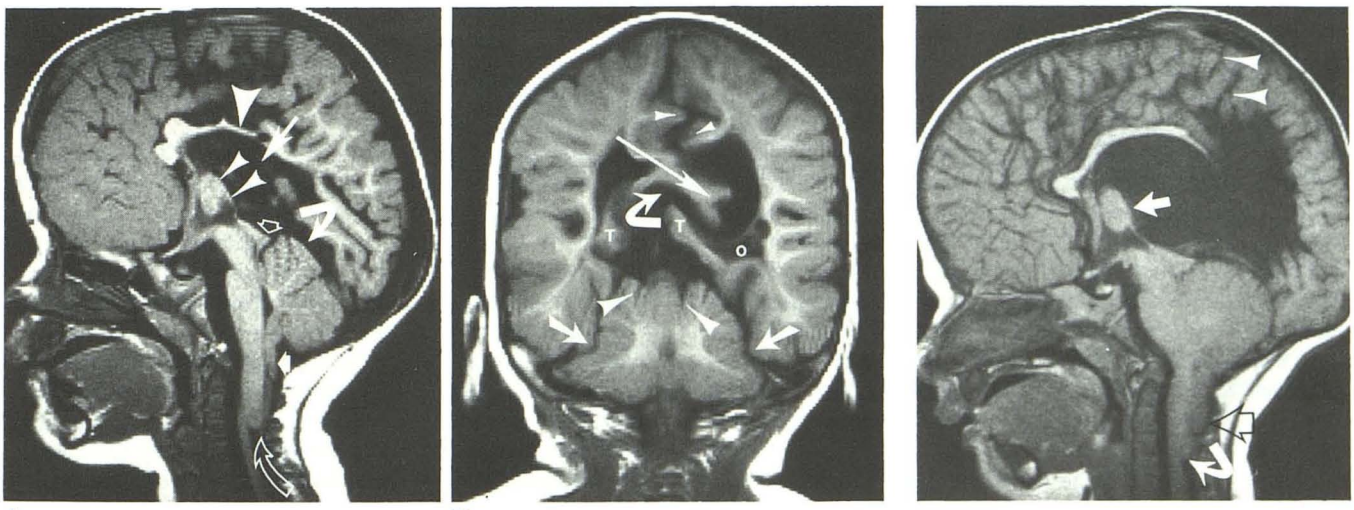

A B

Fig. 3.—*A*, Body of corpus callosum is deformed and markedly thinned (*large arrowhead*). Splenium is absent. Cavum velum interpositum (*long straight arrow*) is markedly dilated displacing third ventricle anteriorly (*small arrowheads*) and communicating with enlarged superior cerebellar cistern (*solid curved arrow*). Tectum is beaked (*open arrow*). Aqueduct is not seen, and fourth ventricle inferiorly is seen extending through foramen magnum. Both inferior vermial peg (*short solid arrow*) and cervicomedullary kink (*open curved arrow*, group 3a) are present.

B, Coronal view immediately posterior to corpus callosum. Absence of falx allows medial interhemispheric gyri to interdigitate (*small arrowheads*). Note enlarged supracerebellar cistern communicating superiorly and laterally (*curved arrow*) with anomalous interhemispheric cistern. Lobules of posteromedial temporal lobes indent cistern medially (T). Note also indentation of left medial occipital gyrus (cingulate isthmus?) into interhemispheric cistern (*long straight arrow*). Left occipital horn (o) is inferiorly displaced. Cerebellum, indented by low tentorium (*shorter straight arrows*), herniates superiorly. Two sagittally oriented sulci are seen on superior surface of cerebellum (*large arrowheads*).

Fig. 4.—Absence of posterior part and splenium of corpus callosum is associated with medial radiating sulci (*arrowheads*). Large interhemispheric CSF-containing space communicates with enlarged cistern velum interpositum. Massa intermedia is enlarged (*straight solid arrow*). Note also beaked tectum, collapsed, nonvisualized fourth ventricle, inferior vermial peg (*open arrow*), and cervicomedullary kink (*curved arrow*).

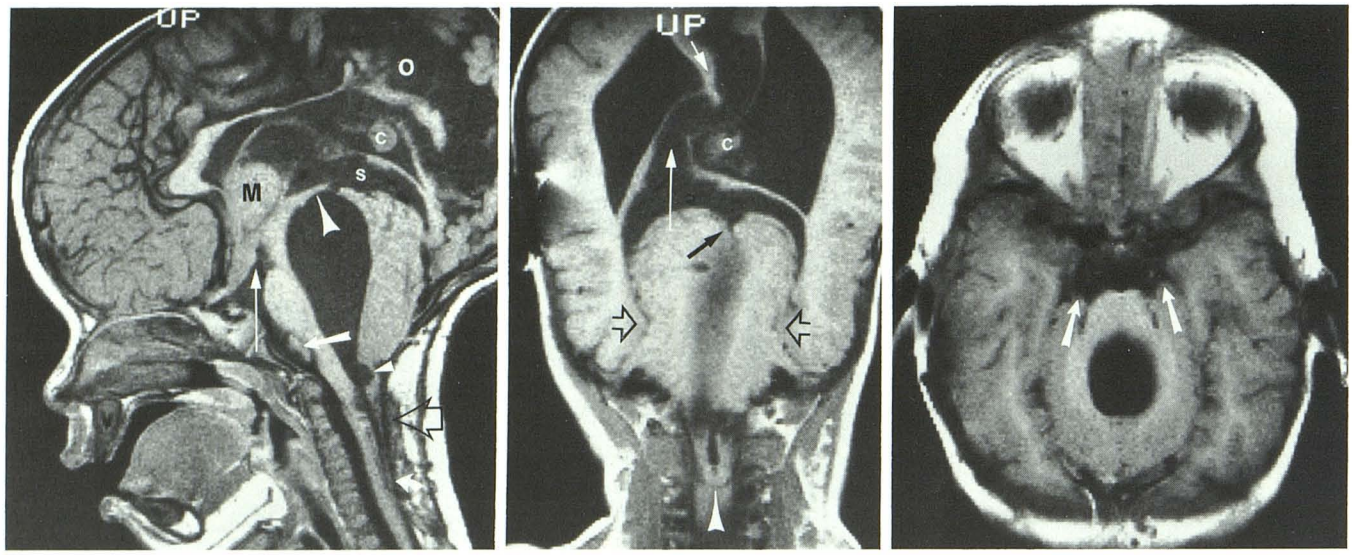

Fig. 5.—*A*, Hypothalamus (*long straight arrow*) is elevated. Note massive enlargement of fourth ventricle (with ventricular diverticuli inferiorly [*small arrowhead*]), apparently communicating superiorly with enlarged supracerebellar cistern. Tectum (*large arrowhead*) is displaced superiorly by fourth ventricle and is beaked. Inferior vermial peg is seen (*open arrow*). Inferiorly, dilated fourth ventricle extends through foramen magnum and is associated with buckling of medulla (*curved arrow*). Cerebellar tissue is seen ventral to pons (*short straight arrow*). Note also thinning of posterior portion of body of corpus callosum (possibly from hydrocephalus) as well as absence of splenium. Supracerebellar cistern (s) and interhemispheric cistern (o) are both enlarged. Choroid plexus of left lateral ventricle (c) extends medially toward midline. Note enlarged massa intermedia (M).

***B*, Coronal view. Note medullary buckle (*arrowhead*) and enlarged supracerebellar cistern communicating with interhemispheric cistern (*long white arrow*). Part of medial occipital gyrus indents cistern (*short white arrow*). Midline cleft is seen on superior surface of cerebellum (*black arrow*). Choroid plexus in left lateral ventricle (c) is indicated. Note also that cerebellum, indented by low tentorium (*open arrows*), herniates superiorly.**

***C*, Axial view. Cerebellar migration is seen on each side of pons (*arrows*). Note enlarged fourth ventricle.**

spaces appeared to communicate freely with a markedly enlarged third ventricle. CT scans of previous hospital admissions for nine of these 11 patients were available for review. All the patients had been previously shunted for hydrocephalus. There appeared to be a relationship between the size of the CCS and the presence of hydrocephalus, with the spaces being smaller or compressed when hydrocephalus was present and larger when the ventricles were effectively shunted. Lobules of the adjacent medial surfaces of the temporal and occipital lobes indented the lateral surfaces of the CCS in many of the patients (Figs. 3 and 5).

Passive widening of the cortical sulci has been described after long-standing decompression of the ventricles of children with hydrocephalus and meningomyeloceles [14]. Naidich et al. [4] reported on the presence of a striking diamond-shaped cistern near the posterior end of the third ventricle in 26% of patients with the Chiari II malformation. They found that the cisterns, as in our cases, were largest in shunted cases. Masters [15] found eight cases of suprapineal recess enlargement in a series of 24 autopsy cases of nonshunted Arnold-Chiari malformations. He found that the enlargement was related to the degree of hydrocephalus, and that when the suprapineal recess was severely dilatated it had ruptured into the subarachnoid space, giving rise to a spontaneous ventriculostomy. In only one of our cases did the third ventricle appear to communicate with the interhemispheric space. Zimmerman et al. [16] also described prominent interhemispheric fissures in 40 of 47 patients with the Arnold-Chiari II malformation, but did not relate the size of the fissures to the presence of hydrocephalus or shunting.

In our cases an association of a widened CCS with partial agenesis of the corpus callosum was seen in all eight patients. Other authors have described marked elevation of the posterior third ventricle into the interhemispheric fissure in patients with agenesis of the corpus callosum [10, 13, 17]. Probst [18] found superior extension of the third ventricle in 40 of 50 children with agenesis of the corpus callosum.

Midline interhemispheric cysts associated with agenesis of the corpus callosum have been described and should also be considered as a possible cause for the enlarged spaces behind the third ventricle in our patients [19–22]. Only in one patient (a patient with a cyst of the ambient cistern) did the borders of the space appear confined, as would be expected with a cyst; but in the remaining patients the CCS instead merged with the adjacent subarachnoid spaces. According to Kendall [10], the posterosuperior extension of the third ventricle in patients with agenesis of the corpus callosum can be sufficiently marked to almost fill the whole length of the interhemispheric fissure, and a greatly enlarged third ventricle may be the cause of most so-called interhemispheric cysts.

We believe as others do that with hydrocephalus, which is almost an inevitable accompaniment of the Chiari II malformation downward herniation of the medial temporal and occipital lobes occurs through the wide tentorium [15]. Because

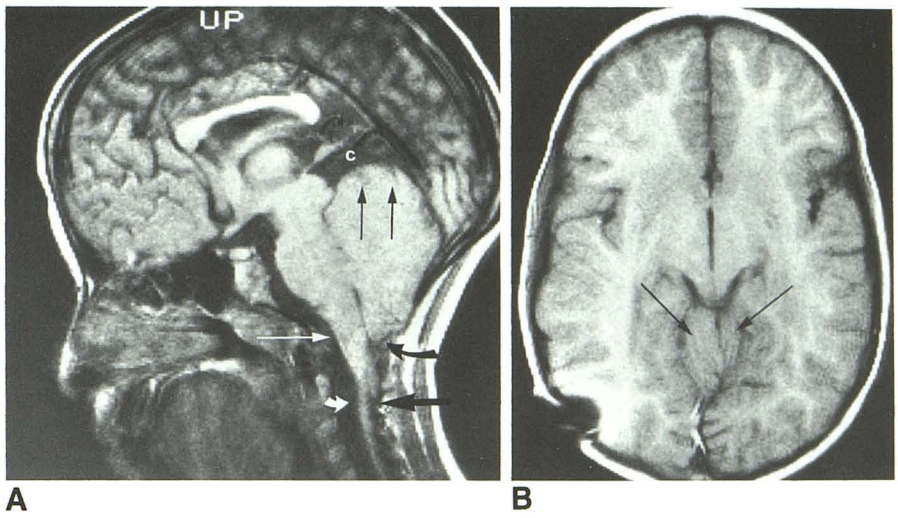

Fig. 6.—Superior vermial sulci (*thin black arrows*) are poorly seen on sagittal scan (*A*). On axial scan (*B*) sulci are faintly seen extending posteriorly (*arrows*), almost in sagittal plane. Subarachnoid space in front of upper cervical cord is wide (*curved white arrow*), but is obliterated at level of foramen magnum (*straight white arrow*). Other features of Chiari II malformation on sagittal scan: enlargement of massa intermedia, bulbous tectum, widening of supracerebellar-CSF cistern (c), nonvisualized aqueduct and fourth ventricle, group 3a cervicomedullary deformity with inferior vermial peg (*curved black arrow*), medullary kink (*thick black arrow*), and concave clivus. Third ventricle, seen on axial view, is not enlarged.

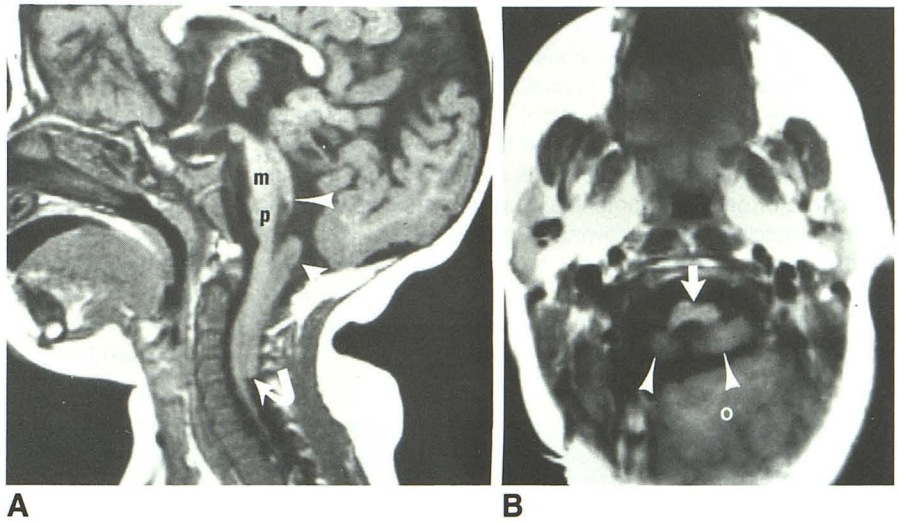

Fig. 7.—*A*, Marked hypogenesis of cerebellum (*straight arrow*), which lies almost completely in upper cervical canal. Tectum (*arrowhead*) is elongated, beaked, and overlies dilated precentral and supracerebellar cistern, which communicates freely through wide incisura with subarachnoid spaces on undersurface of occipital lobes. Note low position of hypogenetic midbrain (m) and pons (p). Clivus is slightly concave.

***B*, Axial scan at level of pons shows hypogenesis of pons anteriorly (*arrow*), cerebellar hemispheric lobules (*arrowheads*) on either side of open fourth ventricle and occipital lobe posteriorly (O). Patient underwent cervical laminectomy. Cerebellum was almost completely located in cervical canal with cerebellar tonsils (*curved arrow*, *A*), forming inferior margin of anomaly. Medullary kink was not seen.**

the tentorium is deficient and its hiatus is enlarged, the medial temporal and occipital lobes are unsupported and subject to severe deformation. After ventricular shunting, the cortex infolds and there is considerable widening of the sulci [14]. The CSF is then directed into the enlarged retromesencephalic cisterns and interhemispheric fissure [23] accounting for the CCS. This phenomenon would be facilitated by the wide tentorial incisura and also the loss of the supporting function of the posterior corpus callosum.

Diencephalon

Third ventricle/massa intermedia.—The third ventricle is generally only mildly dilatated in Chiari II patients [4]. It was normal in 21 of our patients (Fig. 6B) and enlarged in three. The massa intermedia was enlarged in 16 (67%) of our patients (Figs. 4–6), an incidence similar to the 75–90% reported by others [4, 6].

Hypothalamus.—The hypothalamus was elevated and stretched in two patients, neither of whom showed evidence of hypothalamic dysfunction. In one case (Fig. 5A) the stretching was probably caused by the massive accompanying enlargement of the fourth ventricle displacing the midbrain and cerebellum superiorly.

Mesencephalon

Aqueduct.—The aqueduct was not seen or only faintly seen on sagittal images in 17 patients (Figs. 1, 4, 6, and 7). The explanation for the hydrocephalus in the Chiari II malformation—whether aqueduct occlusion is present and whether it is primary or secondary—remains controversial. In a study of 100 brains from children dying with hydrocephalus and myelomeningocele, Emery [24] found that the aqueduct was always anatomically patent but that there was evidence of severe overall shortening of the aqueduct in almost all the cases. In these cases there was severe compression of the aqueduct by pressure from the occipital poles on the brain-

stem. Masters [15] examined 24 autopsy cases of the Chiari II malformation and also concluded that the aqueduct is externally compressed at the level of the tentorial hiatus and that the degree of aqueductal narrowing is proportional to the degree of hydrocephalus. Yamada et al [25] studied 65 Chiari II infants with intraventricular water-soluble contrast agents and found the aqueduct to be anatomically patent in all cases.

We could not relate the nonvisualization of the aqueduct in our 17 patients to the degree of hydrocephalus, since in 14 patients the ventricles were shunted effectively. In none of our patients did the medial temporal lobes appear to compress the midbrain at the level of the aqueduct, and therefore we could not confirm the observations of either Masters [15] or of Emery [24]. In fact, in one nonshunted patient with hydrocephalus, the aqueduct was enlarged on both sagittal and axial images (Fig. 8).

Tectum.—We classified the tectum as having a bulbous appearance (Figs. 1 and 6), in which the two inferior colliculi are elongated sagittally, or a beaked appearance (Figs. 3, 4, 5A, and 7), in which the colliculi are fused to form a single conical mass [6, 7]. The tectum was bulbous in 14 patients and beaked in 10. While we considered that in most cases the tectal deformities were intrinsic to the malformation, it was possible, at least in one patient, that enlargement of the fourth ventricle mechanically caused the tectal deformity (Fig. 9). According to Emery [24], there is an association between the degree of beaking, compression of the brainstem by the dilated ventricles, and narrowing of the aqueduct. We could not relate the appearance of the tectum to the nonvisualization of the aqueduct—a beaked tectum was seen in eight and a bulbous tectum was seen in nine of the 17 patients with nonvisualized aqueducts.

Rhomboencephalon

Cerebellum.—The cerebellar folia of the vermis were either not seen or seen poorly on the sagittal and parasagittal images in 12 patients. In nine patients in whom they were not seen superiorly (Figs. 6A and 8A), diagnostically acceptable axial scans were available in six. In four of these six patients the folia and sulci were faintly seen to extend obliquely posteromedially or directly posteriorly in the sagittal plane (Figs. 6B and 10B). In one patient two parasagittal clefts were seen on each side of the superior vermis (Fig. 3A); in one patient a single cleft was present in the midline (Fig. 5B). In 10 patients the folia were not seen inferiorly.

Cerebellar dysplasia of some form is not uncommon in patients with the Arnold-Chiari malformation, and disorders of neuronal migration (heterotopias and heterotaxias) were described in almost half of the 25 patients in the series of Gilbert et al. [11]. Variend and Emery [26, 27] found that the weight of the cerebellum in children dying with meningomyeloceles was diminished compared with normal children, and that the weight of the cerebellum was inversely proportional to the degree of the hindbrain deformity into the upper cervical canal (Fig. 7). A patient with marked cerebellar and brainstem dysgenesis similar to the one illustrated in Figure 7 was investigated with MR and reported by Yuh et al. [28]. Variend and Emery [29] also analyzed the lobular pattern of the superior surface of the cerebellum and found varying degrees of dorsal angulation and displacement of the primary and postlunate fissures (Fig. 11). In the most severe form of this deformity the cerebellum was split in two with wide separation of the hemispheres. We believe that the nonvisualization of the cerebellar folia in our patients was caused by this dorso caudal angulation of the fissures, as was seen on the axial

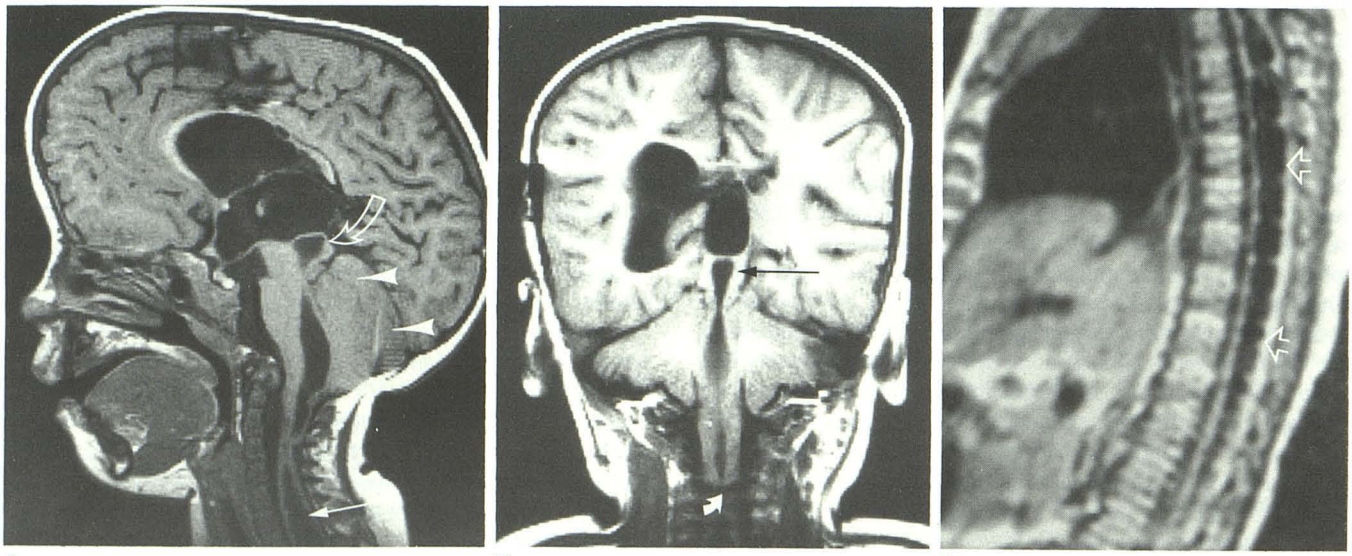

Fig. 8.—*A*, Enlarged fourth ventricle is extending through foramen magnum in association with type 3b cervicomedullary deformity. Note also syringohydromyelia extending inferiorly from level of C5 (*solid arrow*). No folia are identified over surface of vermis (*arrowheads*), even though gyri are identified supratentorially on medial surface of cerebral hemispheres. Aqueduct (*curved arrow*), which is dorsoventrally enlarged in sagittal plane, does not communicate with third ventricle.

***B*, Coronal view shows enlargement of aqueduct in coronal plane (*black arrow*). Note also medullary kink (*white arrow*).**

***C*, Sagittal image of spine (body coil) shows extensive syringohydromyelia extending from T1 to about T12 (*arrows*). Note typical "stack-of-coins" appearance.**

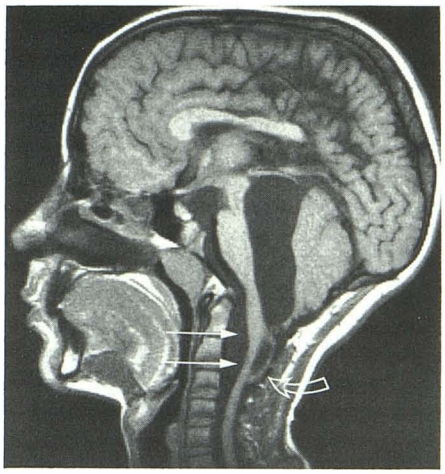

Fig. 9.—Fourth ventricle is markedly dilated and extends into medullary kink (*open arrow*). (Continuity between fourth ventricle and cavity in medulla was confirmed on image 3 mm lateral to this one.) Note wide subarachnoid space ventral to upper cervical cord (*solid arrows*). Upper cervical cord is atrophic (hypogenetic ?) from C2 inferiorly. Note beaked, elevated tectum, possibly deformed because of enlarged fourth ventricle. Fourth ventricle and supracerebellar cistern appear to communicate, perhaps through break in anterior medullary velum. Massa intermedia is enlarged and clivus is concave.

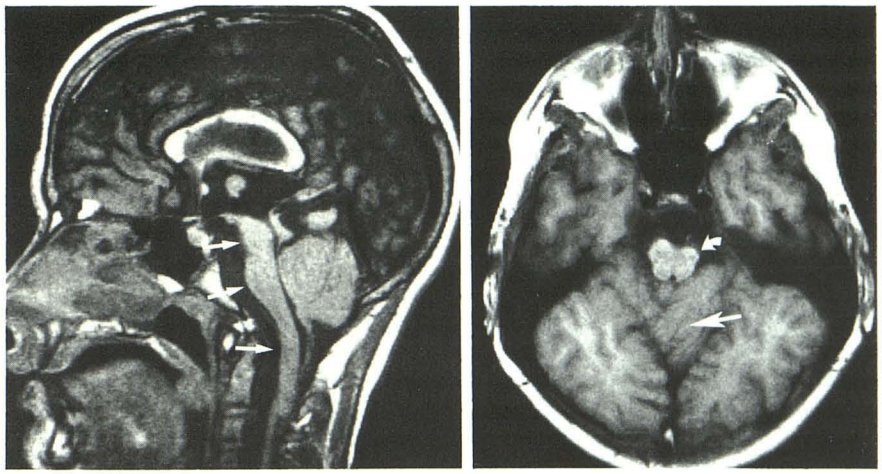

A B

Fig. 10.—Hypogenesis of midbrain, pons, and medulla on sagittal view (*A*) with widening of interpeduncular, prepontine, and premedullary cisterns (*arrows*). On axial scan (*B*), at pontomesencephalic junction, there is hypogenesis of left brachial peduncle (*curved arrow*). Note also poor visualization of superior vermial sulci on sagittal scan, with posterooblique orientation of these sulci on axial scan (*straight arrow*). Anterior cerebellar migration on each side of pons is also evident on axial view. Note inferior vermial spur and medullary kink.

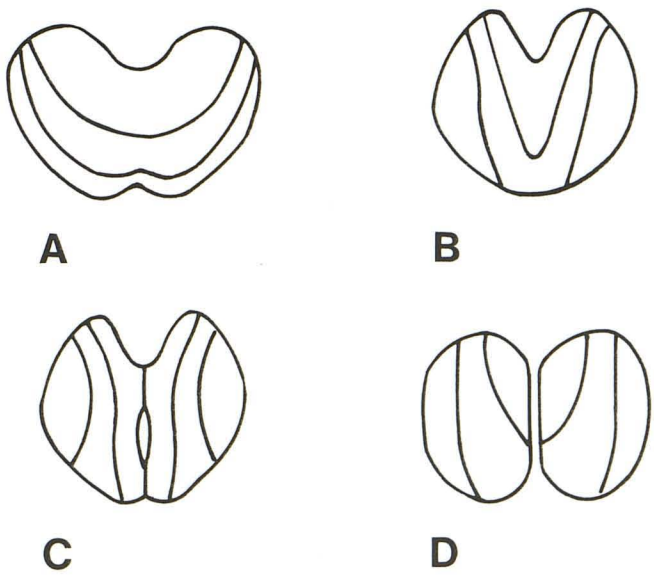

Fig. 11.—Spectrum of distortion of superior surface of cerebellum in myelomeningoceles.

A, Normal shape of superior surface of cerebellum with normal positions of primary and postlunate fissures. (*B–D* are of increasing severity).

B, Moderate V-shaped dorsal displacement of two major fissures and adjacent lobules.

C, With increasing dorsal displacement of two fissures, they become oriented in anteroposterior direction; an aberrant longitudinal fissure extending from precentral fissure through superior vermis is also present.

D, Longitudinal fissure is wide with separation of two cerebellar hemispheres. (Modified from [26].)

views in a number of the patients. Sagittal-plane imaging then would tend to obscure the fissures since they would not lie at right angles to the plane of the scan.

Owing to impaction of the inferior vermis through the foramen magnum, the pyramis, uvula, and nodulus may be compressed with obliteration of the folia. Furthermore, necrosis of these lobules may occur also [26]. Cameron [7] likened the vermial/cerebellar tonsil protrusion through the foramen magnum to a strangulating loop of bowel. The combination of the inferior cerebellar herniation together with the necrosis probably accounts for the nonvisualization of the inferior folia in the 10 patients in our series.

Upward bulging of the cerebellum, which assumes the general configuration of the incisura described by Naidich et al. [4], was also seen on our coronal scans (Figs. 3B and 5B). The same authors described forward migration of parts of the cerebellar hemispheres into the prepontine or premedullary cisterns with envelopment of the brainstem. This appearance, which could also occur at the brainstem level, was seen in 18 of the 24 patients in our series (Figs. 5 and 12).

Vermial pegs.—Inferior vermial pegs or tails were seen extending through the wide foramen magnum dorsal to the medulla and fourth ventricle in 23 of the 24 patients (Figs. 1 and 3–6). In 17 patients the tissue extending through the foramen magnum was pointed in appearance, and in six it was bulbous. On midline sagittal images, none more than 5 mm in thickness, it was assumed that the midline tissue represented the lobules of the inferior vermis, although vary-

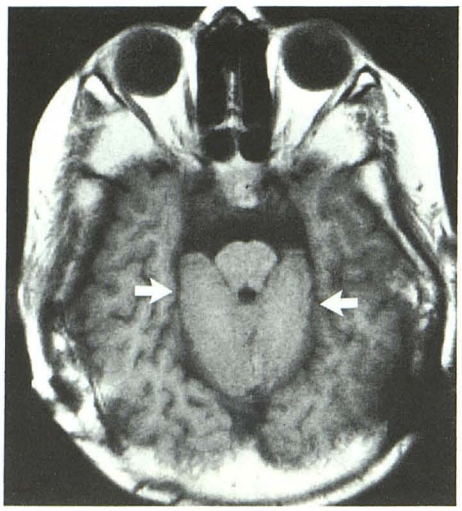

Fig. 12.—Axial scan shows wide margins of tentorial incisura between laterally situated temporal/occipital lobes and medially situated cerebellum (*arrows*). Note also anterior cerebellar migration on each side of pons.

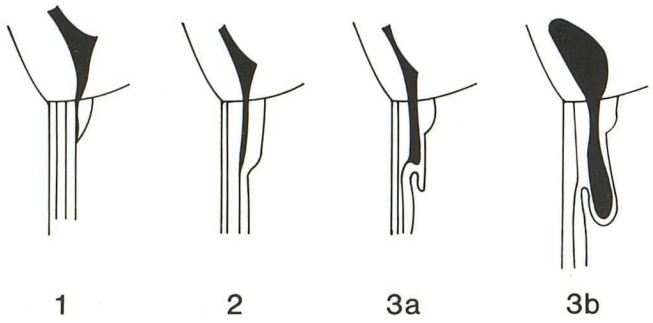

Fig. 13.—Spectrum of cervicomedullary deformities in Chiari II malformation. Anterior is to the reader's left. *Curved line* indicates foramen magnum. *Black shading* indicates fourth ventricle. Diagrams 1, 2, 3a, and 3b represent graded series of increasingly more severe deformities described fully in text. (Modified from [28].)

ing amounts of the inferior cerebellar hemispheres and the tonsils are known to herniate through the foramen magnum as well [30]. In one patient, however, (Fig. 7), the midline tissue was surgically proven to be from the tonsils.

Cervicomedullary deformities.—In analyzing 300 autopsies of children dying with the Chiari II malformation, Emery and MacKenzie [31] grouped the cervicomedullary deformities into different grades of severity. In the mildest form the fourth ventricle had not descended through the foramen magnum, and the only evidence of the abnormality was the upward angle at which the first and second cervical nerve roots exit the cord. In the most severe form the fourth ventricle herniated through the foramen magnum and there was a pronounced medullary kink or spur in the upper cervical canal associated with a cystic cavity contiguous with and arising from the dorsal aspect of the fourth ventricle. The same authors found that the severity of the deformity was directly related to the number of spinal segments involved in the meningomyelocele and also inversely proportional to the length of the dentate ligaments in the upper cervical region.

We modified their classification and grouped our patients as follows (Fig. 13). In group 1, the fourth ventricle and medulla did not descend through the foramen magnum and the sole evidence of a hindbrain deformity was an inferior vermial peg extending through the foramen. In group 2, the fourth ventricle descended vertically through the foramen magnum in front of the vermial peg. In group 3, the medulla was buckled below the cervical cord forming a cervicomedullary "kink," "spur," or "buckle" behind the upper cervical cord. The spur did not extend beyond C4 in any of the cases. The fourth ventricle, which descended through the foramen magnum, was either collapsed (group 3a) or dilated (group 3b). There were six patients with group 1 deformity (one of these patients did not have an inferior vermial peg but had all the other mid and anterior brain features of the Arnold-Chiari deformity). Seven patients had group 2 (Fig. 1) and 11 patients had group 3 abnormalities (eight in group 3a [Figs. 3, 4, 6, and 10] and three in group 3b [Figs. 5, 8, and 9]). Since in all three of the latter patients ventricular shunts had been placed previously for ventricular hydrocephalus, possibly the fourth ventricles had enlarged because of trapping at either end. Yamada et al. [25] found stenotic lesions at the lower portion of the fourth ventricle and at its outlet in the majority of their patients with Chiari II malformation who were studied with water-soluble ventriculography. In our three cases with enlarged fourth ventricles CSF circulatory studies were not carried out.

Pyramids.—Pyramidal hypogenesis (in two patients accompanied with pontine hypogenesis) (Figs. 7 and 10) was seen in four patients. Gilbert et al. [11] found hypoplasia or aplasia of portions of the brainstem, particularly the cranial nerve nuclei, basal pontine nuclei, olivary nuclei, or tegmentum in 12 of 25 children who died with Arnold-Chiari malformation.

Hypogenesis of the pyramids or pontine agenesis appeared to have some clinical correlation with neurologic status in two of the four patients. One child (Fig. 7) is severely disabled with upper extremity weakness and spasticity along with paralysis of the lower extremities; she also has extensive cranial nerve deficits, including vocal cord paresis. Her cerebellum is severely dysplastic. Another child is totally paraplegic. However, six additional children are paraplegic with no demonstrable change in pyramid or stem size, and one child with pyramid hypoplasia has a relatively low-level lesion (L4) and no lateralizing pyramidal extremity deficits. Therefore, we cannot correlate the appearance of the pyramids with clinical symptomatology.

Upper Cervical Canal

Precervical cord space.—We noted a wide subarachnoid space anterior to the upper cervical cord at C1–C3 in nine patients. The space was always present at C2 and varied in level between C1 and C3 (Figs. 6, 8, 9, and 14). Inferior vermial pegs were present in all nine patients. Two patients

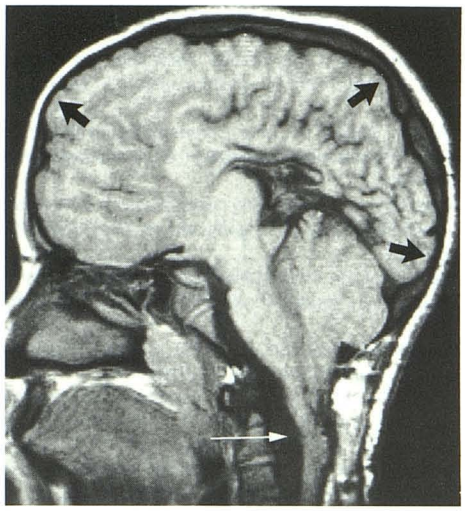

Fig. 14.—Parasagittal scan 3 mm to left of midline shows gyral indentation (*black arrow*) on inner table of skull. Note also wide subarachnoid space anterior to herniated medulla (*white arrow*).

had group 1 deformity, two had group 2, and the other five had group 3 (Figs. 6, 9, and 10). In three of the patients the subarachnoid space at the foramen magnum was obliterated (Fig. 6). In the other six patients (four in group 3, one in group 2, and one in group 1) the subarachnoid space at the foramen magnum anteriorly was normal.

Naik and Emery [32] demonstrated expansion of the upper cervical canal on radiographs of 20 infants with myelomeningoceles. They found that the anteroposterior diameter of the spinal canal from C2 to C4 was significantly larger than the equivalent diameters in 25 normal infants and postulated that this was due to a space-occupying lesion in the upper cervical canal such as would be found with the Chiari II malformation.

While we could not measure the anteroposterior diameters of the spinal canal in our cases, we would postulate that the expansion of the canal may not result only from the medullary kink and vermial spur but may also be secondary to medullary and cervical cord hypogenesis with accompanying mesodermal dysplasia of the developing cervical canal permitting the subarachnoid space to expand.

It would be expected that an inferior vermial peg herniating through the foramen magnum would displace the upper cervical cord anteriorly and obliterate the upper cervical subarachnoid space. According to Venes et al. [12] and Park et al. [33], in myelodysplastic children with swallowing difficulty, stridor, and apnea, an important etiologic factor is compression of the brainstem and the spinal cord in the spinal canal. In our patients there appeared to be no definite clinical significance to the finding of an obliterated subarachnoid space at the foramen magnum. One of the three patients with this finding had been believed by several observers to be developing a progressive right-hand weakness, but no cranial nerve, reflex, or definite extremity changes were noted on examination. Another child had long-standing upper- and lower-extremity weakness and spasticity, and at age 11 months underwent surgery for a high thoracic diastematomyelia; however, he has been clinically stable for 9 years. The third patient (Fig. 6) had undergone surgery 6 months before the MR study for rapidly progressing scoliosis caused by cord tethering at the site of the myelomeningocele repair, but there has been no evidence of progressive myelopathy or cranial nerve or upper extremity symptoms. In our entire series, however, only four patients were evaluated by MR during periods of active symptomatology that might be attributed to the Chiari II malformation. The patient in Figure 7 had had progressing vocal cord paresis and upper extremity spasticity since birth. The MR scan was obtained at age 1½ years and was followed by a C1–C5 laminectomy. A fourth ventricle to cervical subarachnoid shunt was placed, the obex was plugged with muscle, and a dural graft was placed across the laminectomy. Two months later there was some improvement in the vocal cord palsy and upper extremity movements. None of the four patients had significant compression of neural structures at the cervicomedullary junction, suggesting that a major aspect of the surgical approach to the patient with a symptomatic Chiari malformation—laminectomy and dural graft for decompression in the upper cervical area—may have limited applicability. Since the number of symptomatic cases in our series is small, however, this finding will need to be confirmed in a larger study of symptomatic children.

Syringohydromyelia.—In both patients who had spine examinations and in one other patient who had only a head and upper spine scan, syringohydromyelia was seen. In the first patient (who previously had surgery for a syrinx at the C1–C3 level), the syrinx extended from C4 to C7. In the second patient the syrinx extended the total length of the cord from C4 to T12 (Fig. 8). In the third patient a syrinx was identified at the C2 level. The reported incidence of hydromyelia is 20–83% [6, 7]. Had MR studies of the spine been performed routinely, we may have seen cord cavitation more often.

Mesodermal

Clival scalloping.—Clival scalloping (Figs. 1, 3, and 5–10) was present in 19 (79%) of the 24 patients. Yu and Deck [34] found clival scalloping in 94% of their patients with the Arnold-Chiari malformation. Similar to the observation made by the latter authors, the scalloping was not related to age and involved the basiocciput not the basisphenoid. Petrous bone scalloping was also seen in the patients with clival scalloping. These changes are thought to be from pressure by the adjacent cerebellum [2]. Because of the difficulty in defining the posterior lip of the foramen magnum, we could not confirm the enlargement of this structure described by others [2].

Falx defects.—Gyral interdigitations (Figs. 3 and 5) indicating falx fenestration were seen in nine of our patients. Partial absence, hypoplasia, and/or falx fenestrations were reported in all 20 cases of Arnold-Chiari malformation studied in one autopsy series [6].

Widening of the tentorium, diagnosed on axial scans by the appearance of cerebellar tissue extending superiorly without the normal tapering appearance caused by the margins of the tentorium, was seen in 15 patients (Fig. 12). On coronal scans,

both the tentorial widening, diagnosed by visualizing the edge of the tentorium indenting the cerebellum, and a low attachment of the tentorium on the occipital bones (Figs. 3 and 5) were defined easily. Widening of the tentorial incisura and an abnormally low attachment of the tentorium to the occipital bone was seen in 19 of 20 cases reported by Peach [6].

Skull defects.—Gyral indentations into the skull were seen in eight of our patients. Usually the indentations involved the occipital bone. Although some prominence of the inner table of the skull may be found normally, the indentations were particularly prominent in the Chiari II patients, particularly into the occipital bone immediately posterior to the foramen magnum (Fig. 14). Lückenschädel, a frequent accompaniment of the Chiari II malformation, becomes unrecognizable after the age of 6 months [35]. The youngest of our eight patients was 2 years old and the oldest was 17; therefore, we could not determine whether lückenschädel was present in our patients. We believe the appearances were caused by calvarial mesodermal dysplasia, which is part of the Chiari II malformation.

The remarkable development of MR imaging allows the detailed illustration of the complete gamut of abnormalities seen in the Chiari II malformation. We found sagittal-plane images to be most informative. By depicting some features of the malformation with a greater frequency than has been reported to date, and by demonstrating features not seen previously, MR has expanded our knowledge of this complex lesion. MR is our procedure of choice for demonstrating the Chiari II malformation.

REFERENCES

1. Friede RL. Dysplasia of cerebellar hemispheric organization. In: Friede RF, ed. *Developmental pathology*. Vienna: Springer-Verlag. **1975**:314–326
2. Naidich TP, Pudlowski RM, Naidich JB, Gornish M, Rodriguez FJ. Computed tomographic signs of the Chiari II malformation. Part I. Skull and dural partitions. *Radiology* **1980**;134:65–71
3. Naidich TP, Pudlowski RM, Naidich JB. Computed tomographic signs of Chiari II malformation. II. Midbrain and cerebellum. *Radiology* **1980**; 134:391–398
4. Naidich TP, Pudlowski RM, Niadich JB. Computed tomographic signs of the Chiari II malformation. III. Ventricles and cisterns. *Radiology* **1980**;134:657–663
5. Naidich TP, McLone DG, Fulling KH. The Chiari II malformation: Part IV. The hindbrain deformity. *Neuroradiology* **1983**;25:179–197
6. Peach B. Arnold-Chiari malformation. Anatomic features of 20 cases. *Arch Neurol* **1965**;12:613–621
7. Cameron AH. The Arnold-Chiari and other neuro-anatomical malformations associated with spina bifida. *J Pathol* **1957**;73:195–211
8. Muller J. Congenital malformations of the brain. In: Rosenberg RN, ed. *The clinical neurosciences*, vol 3. New York: Churchill, **1983**:1–33
9. Gooding CA, Carter A, Hoare RD. New ventriculography aspects of the Arnold-Chiari malformation. *Radiology* **1967**;89:626–632
10. Kendall BE. Dysgenesis of the corpus callosum. *Neuroradiology* **1983**;25:239–256
11. Gilbert JN, Jones KL, Rorke LB, Chernoff GF, James HE. Central nervous sytem anomalies associated with meningomyelocele, hydrocephalus, and the Arnold-Chiari malformation: reappraisal of theories regarding the pathogenesis of posterior neural tube closure defects. *Neurosurgery* **1986**;18:559–564
12. Venes JL, Black KL, Latack JT. Preoperative evaluation and surgical management of the Arnold-Chiari II malformation. *J Neurosurg* **1986**;64:363–370
13. Atlas SW, Zimmerman RA, Bilaniuk LT, et al. Corpus collosum and limbic system: neuroanatomic MR evaluation of developmental anomalies. *Radiology* **1986**;160:355–362
14. Emery JL. Intracranial effects of long-standing decompression of the brain in children with hydrocephalus and meningomyelocele. *Dev Med Child Neurol* **1965**;7:302–309
15. Masters CL. Pathogenesis of the Arnold-Chiari malformation: the significance of hydrocephalus and aqueduct stenosis. *J Neuropathol Exp Neurol* **1978**;37:56–74
16. Zimmerman RD, Breckbill D, Dennis MW, Davis DO. Cranial CT findings in patients with meningomyelocele. *AJR* **1979**;132:623–629
17. Brun A, Probst F. The influence of associated cerebral lesions on the morphology of the Acallosal brain. A pathological and encephalographic study. *Neuroradiology* **1973**;6:121–131
18. Probst F. Congenital defects of the corpus callosum. Morphology and encephalographic appearances. *Acta Radiol [Suppl]* (Stockh) **1973**;331:1–152
19. Solt LC, Deck JHN, Baim RS, Terbrugge K. Interhemispheric cyst of neuroepithelial origin in association with partial agenesis of the corpus callosum. *J Neurosurg* **1980**;52:399–403
20. Swett HA, Nixon GW. Agenesis of the corpus callosum with interhemispheric cyst. *Radiology* **1975**;114:641–645
21. Zingesser L, Schechter M, Gonatas N, Levy A, Wisoff H. Agenesis of the corpus callosum associated with an interhemispheric arachnoid cyst. *Br J Radiol* **1964**;37:905–909
22. Brocklehurst G. Diencephalic cysts. *J Neurosurg* **1973**;38:47–51
23. Roth M. Further observation on the subarachnoid cisterns in space-occupying lesions of the posterior cranial fossa. *Acta Radiol [Diagn]* (Stockh) **1963**;1:620–627
24. Emery JL. Deformity of the aqueduct of Sylvius in children with hydrocephalus and meningomyelocele. *Dev Med Child Neurol [Suppl]* **1974**;16[32]:40–48
25. Yamada H, Nakamura S, Tanaka Y, Tajima M, Kageyama N. Venticulography and cisternography with water-soluble contrast media in infants with myelomeningocele. *Radiology* **1982**;143:75–83
26. Variend S, Emery JL. The weight of the cerebellum in children with myelomeningocele. *Dev Med Child Neurol [Suppl]* **1973**;15[29]:77–83
27. Variend S, Emery JL. The pathology of the central lobes of the cerebellum in children with myelomeningocele. *Dev Med Child Neurol [Suppl]* **1974**;16[32]:99–106
28. Yuh WTC, Segall HD, Senac MO, Schultz D. MR imaging of Chiari II malformation associated with dysgenesis of cerebellum and brain stem. *J Comput Assist Tomogr* **1987**;11:188–191
29. Variend S, Emery JL. The superior surface lesion of the cerebellum in children with myelomeningocele. *Z Kinderchir* **1979**;28:328–335
30. Variend S, Emery JL. Cervical dislocation of the cerebellum in children with meningomyelocele. *Teratology* **1973**;13:281–290
31. Emery JL, MacKenzie N. Medullo-cervical dislocation deformity (Chiari II deformity) related to neurospinal dysraphism. *Brain* **1973**;96:155–162
32. Naik DR, Emery JL. Diagnosis of Cleland-Arnold-Chiari deformity on plain radiographs of the spine. *Dev Med Child Neurol [Suppl]* **1969**;11[20]:78–81
33. Park TS, Hoffman HJ, Hendrick EB, Humphreys RP. Experience with surgical decompression on the Arnold-Chiari malformation in young infants with myelomeningoceles. *Neurosurgery* **1983**;13:147–152
34. Yu HC, Deck MDF. The clivus deformity of the Arnold-Chiari malformation. *Radiology* **1971**;101:613–615
35. Kruyff E, Jeffs R. Skull abnormalities associated with the Arnold-Chiari malformation. *Acta Radiol [Diagn]* (Stockh) **1966**;5:9–24